Uniaxial Stress and Sol Concentration Dependence of the Structure of a Dressed Macroion in a Dilute Electrolyte Solution

J. Swenson* and M. V. Smalley

Department of Physics and Astronomy, University College London, London WC1E 6BT, U.K.

R. K. Thomas

Physical Chemistry Laboratory, Oxford University, Oxford OX1 3QZ, U.K.

R. J. Crawford

Unilever Research, Port Sunlight Laboratory, Quarry Road East, Bebington, Wirral L63 3JW, U.K.

Received: January 6, 1998; In Final Form: May 1, 1998

Vermiculite clay gels in 0.03 M butylammonium chloride solution were studied by neutron diffraction in the Q range 0.02−2.2 Å^{-1}, permitting a determination of both the distance between the clay platelets (the d spacing) and the intermediate-range structure of the interlayer solution. The structure was investigated as a function of the fraction of the clay in the condensed matter system (r) and the applied uniaxial pressure along the swelling axis (p). The d spacing of about 170 Å at zero pressure and $r \sim 0.01$ reduces dramatically with both increasing pressure and increasing r value without changing the interlayer structure significantly. For $r = 0.39$ a remarkably low d value of about 50 Å was obtained for a gel in equilibrium with a crystalline phase. The existence of such an equilibrium is a counterexample to DLVO theory but well accounted for by Sogami theory. Independent of the pressure, r value, and salt concentration, the clay surfaces are covered by an about 6 Å thick layer of water molecules, and the majority of the butylammonium chains sit outside this water layer and form an approximately 4−5 Å thick layer located 12−16 Å from the center of the clay platelets, giving us a picture of a dressed macroion. Continuum electrical theories of clay swelling can thus only be valid at distances greater than the 35−40 Å thickness of the clay platelet plus adsorbed layers of water molecules and counterions. Further, the results suggest that 35 Å is about the lowest possible d spacing that can be achieved for the gel phase by either increasing the uniaxial pressure toward infinity or using a sufficiently high sol concentration.

1. Introduction

The swelling of vermiculites in aqueous solutions is an anomalous phenomenon, which was first reported by Walker.[1] The swelling, which occurs perpendicularly to the crystalline silicate layers, is dependent on the hydrostatic pressure[2] P, temperature[3] T, uniaxial pressure along the swelling axis[4] p, the volume fraction of the clay in the condensed matter system (sol concentration)[5] r, and the electrolyte concentration in the aqueous solution[1−6] c. These studies have shown that the volume of the originally crystalline vermiculites may expand as much as 50 times when they are soaked in aqueous solutions. The resulting gels have usually a sufficiently large distance between the silicate layers (d spacing) that the system can be treated as an ideal one-dimensional colloidal system. Therefore, the one-dimensional nature of swollen vermiculites makes it possible to do structural investigations not otherwise practicable on a three-dimensional colloid. How the thermodynamic variables affect the interlayer structure of the solution in the gel phase is, however, still not investigated. It is essential to obtain a detailed knowledge of the structure of the vermiculite gels as a model system in understanding many important natural and industrial processes, including colloidal interactions,[7] electrode reactions,[8] and membrane activity and stability.[9]

In a recent paper[10] we investigated the interlayer structure of vermiculite gels in $c = 0.1$ M butylammonium chloride solutions at constant T, P, p, and r. The aim was mainly to determine the distribution of the counterions in the water. For this purpose we used the isotope substitution technique and measured three different samples with 0.1 M H/D salts in D_2O; one vermiculite in 100% H-salt, one in 100% D-salt, and finally the 100% H-salt solution without any clay. The experimental data gave the result that no butylammonium ions are bound directly to the clay surfaces. Instead, the results showed that the clay surfaces are covered by an approximately 6 Å thick water layer and that the "Stern layers" of butylammonium ions are located just outside the water layers, about 7− 11 Å from the clay surfaces. This result throws an interesting light on the Stern layer picture of electrostatic interaction between charged colloids in aqueous electrolytes, in which the majority of the ions should be coordinated to the negatively charged silicate platelets.[11]

In the present paper we aim to investigate how the d spacing and interlayer structure depend on the uniaxial pressure along the swelling axis[4] p and the volume fraction of the clay in the condensed matter system[5] r. Since we are here studying butylammonium vermiculite gels in a lower salt concentration (0.03 M) than in our previous study,[10] we will also be able to determine how the electrolyte concentration in the aqueous solution c affects the interlayer structure. The results will be discussed in conjunction with predictions made from known

S1089-5647(98)00633-6 CCC: $15.00
Published on Web 07/07/1998

theories about electrostatic interactions between charged colloids in aqueous solutions.[12−15]

2. Experimental Section

The vermiculite samples used were from Eucatex, Brazil, with the composition[16] $1.3C_4H_9ND_3-Si_{6.3}Mg_{5.44}Al_{1.65}Fe_{0.6}O_{20}(OH)_4$-$nD_2O$. Crystals about 30 mm^2 in area by 1 mm thick were washed and then treated for about a year with 1 M NaCl solution at 50 °C, with regular changes of solution, to produce a pure sodium vermiculite, following the procedure of ref 17. The completeness of the exchange was checked from the regularity of the *c*-axis peaks in the X-ray diffraction patterns, the *c*-axis spacing for the Na-form being 14.9 Å. To prepare the *n*-butylammonium vermiculite, the Na form was soaked in *n*-butylammonium chloride solution at 50 °C, with regular changes of solution, for about a month. During this process the amount of Na displaced from the crystals was determined by atomic absorption spectroscopy, and the cation exchange capacity of the mineral was found to correspond to a charge density of 1.3 monovalent cations per $O_{20}(OH)_4$ unit. The purity was again checked by X-ray diffraction, the *c*-axis spacing now being 19.4 Å. The crystals were stored in a 1 M *n*-butylammonium chloride solution prior to the swelling experiments.

The gel samples were prepared from the natural crystals using the method described in ref 5. The extent of swelling, and whether or not it occurs, depend on many thermodynamic variables (T, P, p, r, c). In the present experiments we varied p between 0 and 0.2 atm, while T, c, and P were held constant at 10 °C, 0.03 M, and 1 atm, respectively. In the uniaxial stress experiments, the sol concentration was $r = 0.0065$, but we also performed experiments at $r = 0.062$ and $r = 0.39$, where T, c, P, and p were held constant. In the former case we had just slightly more solution than required for full swelling, and in the latter case the amount of solution was not enough to allow full swelling.

For the uniaxial stress experiment a crystal was trimmed to an approximately rectangular shape with cross-sectional area $A = 7.5 \times 4.5$ mm $= 3.4 \times 10^{-5}$ m^2. The initial volume fraction occupied by the clay was $r = 0.0065$, and since the free swelling was approximately 9-fold (from about 20 to 180 Å), the final volume fraction was about 0.06. A sliver of the swollen gel less than 1 mm thick was then placed in the uniaxial stress cell illustrated in Figure 1. The internal dimensions of the quartz cell were $30 \times 5 \times 2$ mm, with the clay gel loaded parallel to the 30×5 mm faces. The outer cell was filled with the solution in which the gel had previously been soaking, both to maintain equilibrium and to lubricate the process of sliding the clay gel between the quartz faces. This was a delicate process, it being necessary not to subject the gels to any squeezing force because they are very easily compressed from their equilibrium zero stress spacings.

The device illustrated in Figure 1 was a prototype apparatus that relied for its operation on the bending of a quartz plate of 1.0 mm thickness which was used to apply force to the sample directly. The bending of the plate was measured with a strain gauge. Its response was linear up to a force of 0.7 N, approximately equal to the maximum force applied in the present experiment, corresponding to a uniaxial stress of about 2×10^4 N m^{-2} or 0.2 atm. The device was mounted on a standard goniometer head for the neutron diffraction experiments on the D16 diffractometer at the Institute Laue−Langevin (ILL), Grenoble, France. The diffractometer has been described in detail elsewhere.[18]

To reduce the incoherent and inelastic scattering from the samples, we used fully deuterated water in all cases. This is important since the majority of the scattering observed is from the water. We also prepared a sample where all the H in the butylammonium chains was deuterated, in order to make use of the large difference in scattering length between H and D ($b_H = -3.74$ fm and $b_D = 6.67$ fm) and investigate the distribution of the butylammonium ions in the interlayer solution.

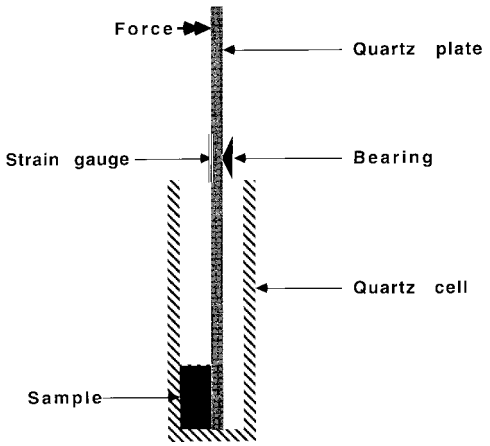

Figure 1. Schematic illustration of the principle of operation of the prototype uniaxial stress cell used in the current experiments. The internal dimensions of the quartz cell were $30 \times 5 \times 2$ mm.

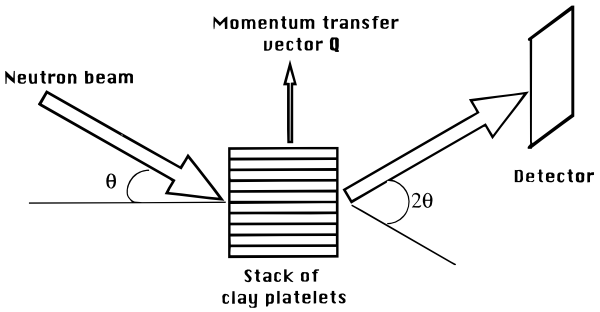

Figure 2. Illustration of the $\theta-2\theta$ geometry of the neutron diffraction experiments on the D16 diffractometer at ILL. In order to ensure that the momentum transfer vector **Q** was always perpendicular to the clay platelets, the samples were rotated from 5° to 52° in steps of 1° when the scattering angle was increased from 10° to 104° in steps of 2°. Spectra were recorded for each scattering angle and thereafter combined.

The samples were oriented such that the clay platelets were perpendicular to the momentum transfer vector **Q**, described as $Q = Q_z$. The geometry of the experimental setup is shown in Figure 2. First, we used a sample−detector distance of 1.0 m and kept the detector position fixed at the scattering angle $2\theta = 5°$ (the detector covered about 9° at a sample−detector distance of 1.0 m), in order to measure the lowest Q range with a good resolution. Thereafter, the sample−detector distance was reduced to 0.5 m, and spectra were recorded separately for each scattering angle, which was increased from 10° to 104° in steps of 2° (the detector covered now about 18°), and also for monitors in the incident and transmitted beam. The incident wavelength was 4.53 Å. The data from the different scattering angles were then combined and corrected for background and container scattering and absorption. They were then normalized to a proper structure factor for the *z* direction (perpendicular to the clay platelets), $S(Q_z)$. For each Q value, we used only the detector cells which gave mutually consistent results from the overlapping frames.

The structure factor obtained from each sample was in some cases Fourier transformed to obtain a total neutron weighted one-dimensional pair correlation function along the *z* axis

$$G(r_z) = \frac{2\sum_{i=1}^{n} c_i b_i^2}{\pi\rho^0(\sum_{i=1}^{N} c_i b_i)^2}\int_0^\infty (S(Q_z) - 1)\sin(Q_z r_z)\,dQ_z + 1 \quad (1)$$

where ρ^0 is the average number density and c_i and b_i are the concentration and neutron scattering length of atom i, respectively.

3. Results

In Figure 3 we show the low-Q range neutron data of the vermiculite in 0.03 M H-butylammonium chloride solution ($r = 0.0065$) for different applied uniaxial pressures. The result confirms earlier investigations[5,19,20] that the average interclay layer spacing (d spacing) decreases with increasing applied pressure. The position of the first-order Bragg peak (see Table 1) corresponds to a d spacing of about 170 Å, which decreases continuously with increasing pressure to about 80 Å at 0.2 atm. We first study how the applied pressure affects the width and maximum intensity of the first-order Bragg peak (see Table 1). The ratio between the width, ΔQ_1, and the position, Q_1, of the peak seems to decrease with increasing pressure in the whole pressure range, although the rate of the decrease is much more rapid for low pressures. The change of the maximum intensity of the first-order Bragg peak shows an anomalous behavior. First, it increases for increasing applied pressure, and then at an intermediate pressure the trend is changed and the intensity starts to decrease again. Possible reasons for these systematic intensity changes will be discussed below.

Applied uniaxial pressure also affects the higher Q range of the structure factors, which involves intermediate-range correlations within the solution and correlations between the clay platelets and the solution. In Figure 4 we show the structure factors in the Q range 0.2−2.1 Å^{-1} for the vermiculite in 0.03 M D-butylammonium chloride solution at zero pressure, and the same sample as was shown in Figure 3 for the applied pressures 0, 0.04, and 0.07 atm, respectively. Thus, the Bragg peaks due to the interplatelet correlations are located at lower Q values than are shown in this figure.

Considering that the clay platelets occupy only about 1% of the total sample volume and that the remaining part is the weak n-butylammonium chloride solution (located either between or outside the clay platelets), the structural features and differences are interestingly large. The structure factor of the vermiculite in the 0.03 M D-salt solution shows a broad weak peak at about 1.0 Å^{-1} and a strong peak located at about 2.0 Å^{-1}, while all the three structure factors of the vermiculite in the 0.03 M H-salt solution show strong peaks at about 0.4 and 2.0 Å^{-1} and weaker peaks around 0.7 and 1.1 Å^{-1}. Thus, there are large differences between the structure factors of the vermiculites in D- and H-salt solutions. Furthermore, it is evident from the structure factor of 0.1 M butylammonium chloride in D_2O (given in ref 10) that the scattering contribution from butylammonium ions located outside the clay gels is very small.

The applied uniaxial pressure on the sample in H-salt solution has almost no effect on the positions of the peaks. The intensity of the strong peak at about 2.0 Å^{-1} shows only a minor pressure dependence (it is mainly the width of the peak which seems to change), while the intensities of the other peaks change significantly with the applied pressure. The intensity of the peak at about 0.4 Å^{-1} increases continuously with increasing pressure, and at a pressure of 0.07 atm the top of the peak shows a remarkable sharpness. The position of the peak corresponds to a real-space characteristic length of about $2\pi/Q_{peak} \approx 16$ Å. For the peaks located at about 0.7 and 1.1 Å^{-1} the intensity is largest, as for the first-order Bragg peak due to the interclay platelet correlation, for an intermediate pressure of 0.04 atm. The structure factor of the vermiculite in 0.03 M D-salt solution seems rather featureless, but one should note its much higher intensity compared to the vermiculite in H-salt solution in the Q range around 0.2−0.3 Å^{-1}. This is evident in Figure 5, which shows the difference curve $\Delta S(Q_z)$ between the structure factors of the vermiculites in D- and H-salts. The corresponding difference curve for vermiculites in 0.1 M salt solutions[10] is also shown for comparison. Both difference curves show a relatively strong peak at about 0.25 Å^{-1} and smaller peaks (or shoulders) at about 0.55 and 0.8 Å^{-1}. The overall shapes of the two curves are similar. For $Q < 0.2$ Å^{-1}, the curves are strongly negative due to the fact that the Bragg peaks arising from the interplatelet correlations are much stronger for the vermiculites in H-salt, where the scattering contrast between the clay layers and the interlayer solution is greater.

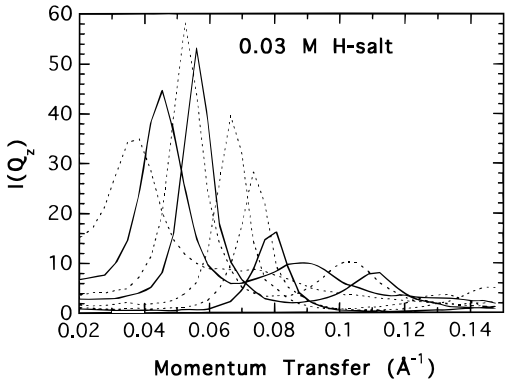

Figure 3. Low-angle neutron diffraction data measured in the z direction (perpendicular to the clay platelets) for a $c = 0.03$ M butylammonium vermiculite gel at $r = 0.0065$, $T = 10$ °C, and seven uniaxial pressures. Note the systematic variation of the intensity and width of the (001) reflection as a function of the applied pressure. The d values derived from the approximate relation $d = 2\pi/Q_1$ and the corresponding pressures are given in Table 1.

TABLE 1: Peak Positions, Intensities, and Widths and Calculated d Spacings as a Function of Applied Uniaxial Pressure for a $c = 0.03$ M Butylammonium Vermiculite Gel at $r \sim 0.01$ and $T = 10$ °C[a]

p (atm)	Q_1 (Å^{-1})	$I(Q_1)$	ΔQ_1 (Å^{-1})	$\Delta Q_1/Q_1$	d (Å)
0†	0.0372	33.3	0.0209	0.562	169
0.011*	0.0372	35.2	0.0211	0.567	169
0.014	0.0383	25.9	0.0215	0.561	164
0.018	0.0409	24.0	0.0213	0.521	154
0.022	0.0419	40.0	0.0167	0.399	150
0.025*	0.0453	44.7	0.0152	0.336	139
0.030	0.0489	48.3	0.0140	0.286	128
0.039*,†	0.0523	58.1	0.118	0.226	120
0.042	0.0523	53.9	0.111	0.212	120
0.052	0.0550	51.7	0.110	0.200	114
0.055*	0.0559	53.1	0.108	0.193	112
0.074†	0.0605	49.4	0.107	0.177	104
0.096	0.0655	41.5	0.104	0.159	96
0.11*	0.0677	39.4	0.110	0.162	93
0.13	0.0710	37.0	0.111	0.156	88
0.17*	0.0734	28.1	0.107	0.146	86
0.18*	0.0796	16.6	0.117	0.147	79
0.22	0.0817	16.6	0.115	0.141	77

[a] The asterisks mark the pressures for which the low-angle diffraction data are shown in Figure 3. The daggers mark the three points for which wider angle diffraction data are shown in Figure 4.

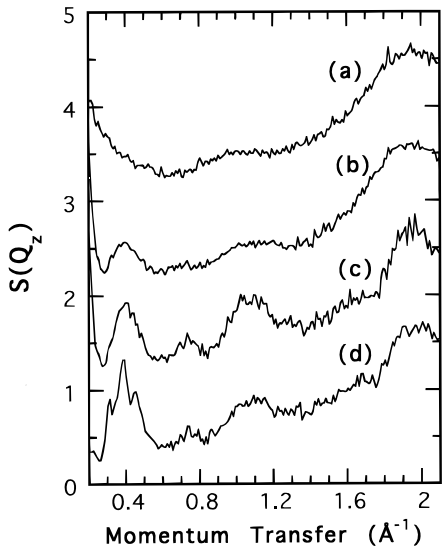

Figure 4. Structure factors $S(Q_z)$ in the range $0.2 < Q < 2.1$ Å^{-1} obtained from neutron scattering patterns of 0.03 M butylammonium vermiculite gels at $r = 0.0065$ and $T = 10$ °C. (a) D-salt at $p = 0$. (b), (c), and (d) H-salt at $p = 0$, 0.04, and 0.07 atm, respectively. Consecutive curves are shifted vertically for clarity.

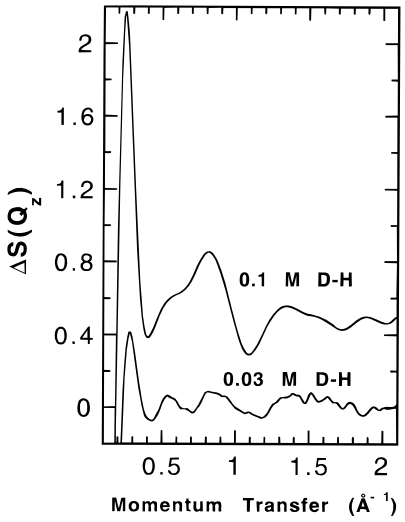

Figure 5. Difference curve $\Delta S(Q_z)$ between the vermiculites in D- and H-salt solutions at $c = 0.03$ M (lower curve), obtained by subtracting the data shown in Figure 3b from that in Figure 3a. As a comparison, the corresponding difference curve for vermiculites in 0.1 M salt solutions[10] is also shown (upper curve).

To simplify the interpretation of the structural features observed in reciprocal space, the structure factors were Fourier transformed to atomic pair correlation functions, $G(r_z)$, measured in the direction perpendicular to the clay platelets (in the z direction). The structural correlation functions $r(G(r_z) - 1)$ derived from $G(r_z)$ are shown in Figure 6 for the same vermiculites and the same uniaxial pressures as shown in Figure 4. It should be noted that the structural features in the region $0 < r_z < 5$ Å are very approximate due to the low maximum Q value of 2.2 Å^{-1} and will therefore not be discussed in this paper.

All the correlation functions show a sharp peak at about 7.5 Å, which due to its generality and r value we interpret as mainly arising from the correlation between the two surface oxygen layers within the clay platelets. All the other small sharp peaks are, at least partly, ripples produced in the Fourier transformation procedure due to the low maximum Q value of the structure

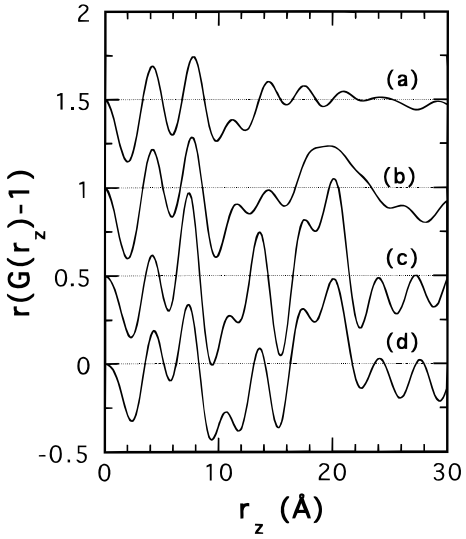

Figure 6. Atomic one-dimensional pair correlation functions $G(r_z)$ derived from the structure factors shown in Figure 4, presented as $r(G(r_z) - 1)$. (a) to (d) are as described in the caption to Figure 4. Consecutive curves are shifted by 0.5 for clarity.

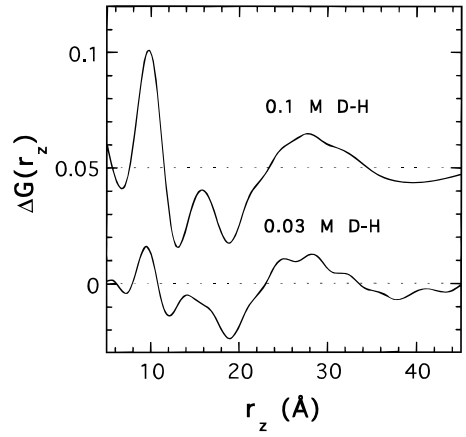

Figure 7. Difference pair correlation functions $\Delta G(r_z)$ obtained by Fourier transformation of the difference structure factors $\Delta S(Q_z)$. The upper curve is shifted by 0.05 for clarity.

factors. However, the negative region $9 < r_z < 13$ Å in all of the functions $r(G(r_z) - 1)$ is real, as well as the broad peak in the range $17 < r_z < 22$ Å and the negative region $23 < r_z < 30$ Å for the vermiculite in H-salt solution at different uniaxial pressures. Most of the structural features are strongest at the intermediate pressure of 0.04 atm, which is in agreement with the observations in reciprocal space. The correlation function of the vermiculite in D-salt solution is almost flat for $r_z > 13$ Å.

In Figure 7 we show the Fourier transforms of the difference curves $\Delta S(Q_z)$ shown in Figure 5. These real space difference functions $\Delta G(r_z)$ give us the correlations due to the replacement of H ions by D ions. The correlations involving butyl chains will give positive contributions to $\Delta G(r_z)$, while correlations involving D_2O give negative contributions. It is evident in Figure 7 that both $\Delta G(r_z)$ show clear peaks at about 10 and 15 Å and a broad positive region around 23−34 Å. One should also note the broad dips (negative contributions) in the ranges 12−23 and 35−45 Å.

We also investigated how the structure factor changes with the volume fraction r of the clay in the condensed matter system, at $p = 0$. Figure 8 shows the low-Q range ($0.02 < Q_z < 0.15$ Å^{-1}) of the structure factor of the vermiculite in 0.03 M

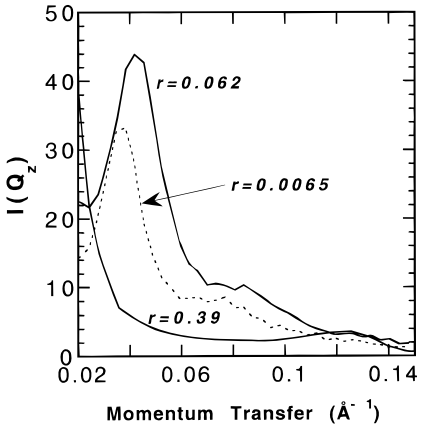

Figure 8. Low-Q neutron data $I(Q_z)$ obtained at $c = 0.03$ M and $p = 0$ as a function of sol concentration r.

H-butylammonium chloride solution for $r = 0.0065$, $r = 0.062$, and $r = 0.39$, respectively. In Figure 9a,b the higher Q range of the same structure factors are shown. Two interesting results are evident from these figures. First, Figure 8 shows that the d spacing decreases with increasing fraction of clay, although there is enough solution to allow full swelling for the two samples with lower clay volume fractions. Second, for $r = 0.39$ one obtains a d spacing of about 50 Å, which should be the average interlayer distance if all the solution was in between the clay platelets. However, Figure 9b shows clearly that the crystalline phase, with its normal d spacing of about 19.4 Å, is also present. Figure 9a and the diffuse scattering in Figure 9b show no evidence for changes in the interlayer structure as a function of r, although the presence of two phases makes the analysis difficult for $r = 0.39$. Most of the differences in the data for $r = 0.0065$ and $r = 0.062$ can, however, be explained by the larger volume of the vermiculite gel in the neutron beam in the latter case.

4. Analysis

In presenting the results, we have used the approximation that the momentum transfer vector Q was perpendicular to the clay platelets. However, in interpreting the low-Q data in Table 1, it is essential to take the finite mosaic spread of the gels into account. Before choosing a sample for the uniaxial stress experiment, the d spacings and mosaic spreads of nine gels were measured by taking a rocking curve on the (001) reflection due to the interplatelet correlation, the average values being 174 Å and 5.8°, respectively.[4] The gel studied had typical values. The application of stress may cause this mosaic spread to sharpen at low stresses. Since it is likely that the depth and sharpness of the potential well will increase with increasing stress and decreasing d spacing, we may also expect the d spacing to become more regular with increasing stress. The observation that the first-order Bragg peak is getting sharper with increasing uniaxial pressure (see Figure 3) can doubtless be explained by a combination of these two effects. However, in the prototype apparatus used, the stress was not purely uniaxial because a bending force was applied to the quartz plate transmitting the stress (see Figure 1). Although the shear stress component was small, the clay layers slip very easily over each other in the gel phase, and it is possible that small amounts of gel were squeezed upward out of the beam during the course of the experiment, which was carried out over a period of 2 days. The bending operation of the quartz plate may also bring about a displacement in the average orientation of the sample with respect to the beam at high stresses, and a combination of these two experimental

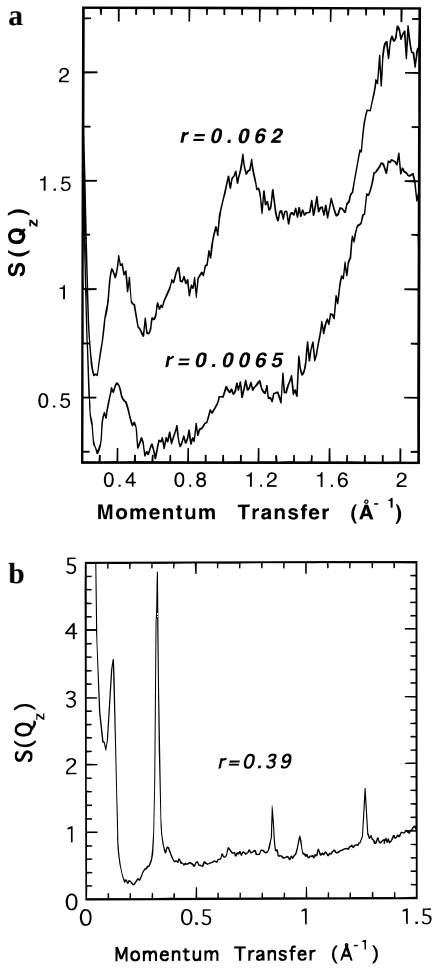

Figure 9. Structure factors $S(Q_z)$ obtained at $c = 0.03$ M and $p = 0$ as a function of sol concentration r in the higher Q range. (a) shows the data for $r = 0.062$ and $r = 0.0065$ and (b) the data for $r = 0.39$. In (b), the scale has been expanded to show the more intense peaks due to the $d = 19.4$ Å crystalline phase of the vermiculite.

effects probably accounts for the observation that the intensity of the Bragg peak starts to decrease at high pressures.

The tilting of the clay layers may also explain the decrease in intensity of some of the structural features observed in the higher Q range at high pressures (see curves c and d in Figure 4). The origins of the peaks in the higher Q range of the structure factors are not immediately obvious, although it is very likely that the peak at about 2 $Å^{-1}$ is due to correlations within the water since its position and shape coincide with the first diffraction peak in pure D_2O. To make a safe interpretation of the other peaks, one needs to do a careful and simultaneous analysis of the data from the vermiculites in H- and D-salt solutions and the data obtained for the pure solution. Such a analysis has previously been performed for vermiculites in 0.1 M H and D-butylammonium chloride solutions[10] and is briefly repeated below to make the present analysis intelligible. The eventual differences and similarities between the results for the two different salt concentrations are, however, interesting to investigate, as well as the effect of the applied uniaxial pressure.

The difference functions in Figures 5 and 7 have not been shown previously for any salt concentration. These figures show that the structural dependence on the salt concentration is very weak. For both salt concentrations, it is evident (see also the detailed analysis in ref 10) that the intense peak at about 0.25 $Å^{-1}$ in $\Delta S(Q_z)$ and the broad peak around 23−34 Å in $\Delta G(r_z)$ are due to correlations between butyl chains. Thus, it is very

likely that a large fraction of the butylammonium ions are located approximately 12−17 Å from the center of the clay platelets. Furthermore, the broad negative contributions in $\Delta G(r_z)$ at about 12−23 and 35−45 Å (see Figure 6) indicate that the approximately 5 Å thick layer of butylammonium ions is surrounded by pure water on both sides. This confirms our previous conclusion that every clay sheet is coated with about a 6 Å thick water layer (corresponding to two layers of water molecules)[10] and further implies that a second water layer is located on the other side of the butylammonium ions approximately 17−22 Å from the center of the ∼10 Å thick clay layers.

From the correlation functions $r(G(r_z) - 1)$ shown in Figure 6 it seems likely that the density of the water molecules closest to the clay platelets is less than the density of bulk water, while the water molecules closest to the butylammonium ions seems to have slightly higher density and/or be more orientationally ordered than bulk water. A natural interpretation of this analysis is that one layer of water molecules is adsorbed at the clay surface and that a second layer is strongly bound to the butylammonium ions. The structural ordering and density of these two water layers may, thus, differ significantly. Within this schema, it would also be expected that there would be a stongly bound water layer on the solution side of the counterion layer, and this fits with the dip in $\Delta G(r_z)$ at about 35−45 Å. This gives us a structural picture of a "dressed macroion" in which the bare clay platelet thickness is extended to approximately 40 Å by successive adsorbed layers of water molecules, counterions, and further partially ordered water molecules. We thus show that the lowest value for the *d* spacing at which primitive theories, treating the solvent as a uniform dielectric continuum, could be valid is further out than we suggested in our previous paper, from 28 Å to at least 35 Å.

We now focus on how the applied uniaxial stress affects the structure of the solution. The structure factors shown in Figure 4 and the real space correlation functions $r(G(r_z) - 1)$ shown in Figure 6 indicate an increased ordering with increasing pressure (at least for pressures up to about 0.04 atm) in the solution closest to the clay platelets. The correlation between the water molecules bound to the butylammonium ions (on the "inner" side closest to a clay surface) on each side of a clay sheet gives rise to the peak at about 0.4 $Å^{-1}$ in the structure factors of the vermiculite in H-salt solution and the broad peak in the range $17 < r_z < 22$ Å of the corresponding $r(G(r_z) - 1)$ functions. The intensities of these peaks increase and get narrower in the case of real space with increasing pressure, which indicates that the distance from the center of the clay platelet to the water layer on each side gets slightly more well-defined. The average distance is, however, maintained. It also seems that the low-density water layer closest to the clay surface retains its low density and, therefore, probably also its structure even at the highest pressure. Since the water−water correlation gets slightly more well-defined, it is also likely that the layer of butylammonium ions gets slightly narrower. The main conclusion to be drawn is that the dressed macroion structure of the clay plate plus its two absorbed layers of water molecules and one adsorbed layer of counterions is constant with respect to uniaxial stress.

Figures 8 and 9 show how the structure factor changes with the volume fraction *r* of the clay in the condensed matter system. In Figure 8 it is evident that the *d* spacing decreases with increasing fraction of clay, although there is enough solution to allow full swelling for the two samples with lowest clay fractions. The reason for this is that salt trapped inside the crystals during the preparation process is released into the external solution during gel formation, increasing the salt concentration. The concentration in the butylammonium chloride crystals is approximately 0.1 M, with wide sample-to-sample variability.[5] At $r = 0.062$, this gives an additional background electrolyte of 0.0062 M or $c = 0.036$ M overall, which is about 20% higher than the added salt concentration. Previous observations[1,3−5,19−22] and electrical theory[6,23,24] both suggest that the interplate separation in the gel phase is inversely proportional to $\sqrt{c}$, so a 10% contraction in this case is entirely predictable.

For the highest clay fraction ($r = 0.39$) the trapped salt leaching out of the crystals gives an additional background electrolyte of 0.039 M or $c = 0.069$ M overall, still well within the range of stability of the gel phase at $T = 10$ °C for unrestricted swelling at low *r*. There is not enough solution to allow full swelling in this case because the total volume of the solution corresponds to an average *d* spacing of about 50 Å, provided that all solution is inside the gel. This *d* spacing of 50 Å is, in fact, exactly what we observe in Figure 8. The result may at first sight be obvious, but it is not when we also observe in Figure 9b that we have a significant part of the clay in its nonswollen crystalline phase. It is impossible to estimate accurately the relative quantities of the two phases in equilibrium, but we note that the first-order crystalline peak is generally an order of magnitude more intense than the gel peak for similar sized samples,[3] so the fraction in the crystalline phase was probably comparatively small. The observation of the *d* spacing in the gel phase being exactly as expected for swelling of all the sample was therefore probably accidental, an artifact caused by the problem of mixing the whole crystalline vermiculite with the solution during the sample preparation. Several crystals of total mass 12.2 g were placed in a beaker, and 10 cm^3 of solution was added. Some of the solution may have become trapped between different gel stacks, leading to a higher sol concentration *r* in the gel stacks. For *r* in the range between 0.4 and 0.5, the average maximum *d* spacing is between 50 and 40 Å. In the latter case the coexistence of 20 and 50 Å phases is understandable on space-filling grounds, but it is still a remarkable phenomenon, as discussed below.

It was also remarkable that the diffuse scattering in Figure 9b is so similar to that in Figure 9a, indicating that the dressed macroion structure is essentially the same at 50 Å as in the range 80−170 Å covered by the uniaxial stress results. This is an important result, as discussed below.

5. Discussion and Conclusion

The main result to emerge from the study is the invariance of the dressed macroion structure with respect to changes in the variables *r*, *c*, and *p*. In every case studied the clay surface is covered by two layers of water molecules, then a layer of counterions, giving a block of 30−35 Å thickness. If we interpret the "outer" water layer as being associated with the counterions, it is logical to expect a further partially ordered water layer on the solution side of the counterion layer, and although the evidence is inconclusive on this point, there are indications in the data that this is indeed the case. This gives rise to a structural block 35−40 Å thick, which probably represents the smallest *d* spacing possible for the gel phase. At higher *r*, *c*, and *p* values, we may expect it to be possible to produce such a spacing but then to produce collapse into the $d = 19.4$ Å crystalline phase.

The other important new result was the coexistence of the gel and crystalline phases at the high volume fraction $r \cong 0.4$.

Previous studies[2−6] for $r < 0.1$ have shown a sharp phase transition between the two phases, and it has been noted[24,25] that the existence of such a transition is a counterexample to the DLVO theory of colloid stability, in which the gel phase could only be kinetically stable. The new findings underline this deficiency in the standard theory of colloid stability. In the limited beam time available, it was not possible to perform a systematic study of the temperature dependence of the coexistence curve, but the temperature of the sample was varied and it was found that the intensity of the (001) peak of the crystalline phase decreased by a factor of 3 between $T = 16$ and 0 °C, showing again[2−6] that the gel phase is more stable at low temperatures (at least for $T > 0$ °C). It is evident that the effect of having a low fraction of solution in the system needs to be further investigated.

Although DLVO theory is unable to explain the equilibrium between the gel and crystalline phases and gives an inaccurate prediction for the dependence of the *d* spacing on *c*, both are well accounted for by the Sogami theory of plate macroions.[6,24,25] Indeed, the discovery of an effective "clay layer thickness" of 35−40 Å improves the agreement between the prediction of Sogami theory and the observed *d* spacings. It has been shown that the former predicts spacings of seven Debye lengths for low *r* and low *c*, giving results systematically lower than the observed values. At $c = 0.03$ M, the Debye length is 18 Å and the prediction is $d = 126$ Å. If we add to this the invariant plate thickness, we obtain $d \cong 160$ Å, in good agreement with the data. We therefore believe that electrical theory should be retained as the central theory of clay swelling, but with the following proviso. The observation that a large fraction of the counterions are located approximately 12−16 Å from the center of the clay platelets means that if one wishes to retain the concept of an "outer Helmholtz plane" at which one can define an effective surface electric potential,[6] one must use an effective "clay layer thickness" of 35−40 Å, since the layers of counterions must be included.

The fraction of the total number of butylammonium ions located within the layers about 12−16 Å from the center of the clay platelets is difficult to estimate accurately, mainly due to the limited *Q* range and the partly unknown fraction of the gel in the neutron beam. However, with the assumption that 100% of the sample scattering (the container scattering is subtracted) is from the gel, it is possible to make a rough estimation of the number of butylammonium ions within the layer giving rise to the peak at 25−30 Å in the $\Delta G(r_z)$ shown in Figure 7. From the integrated area of the positive part of that peak in $\Delta G(r_z)$, the fractions of butylammonium ions have been estimated to 46% and 39% for the gels in 0.03 and 0.1 M salt solutions, respectively. If some of the sample scattering was from the external solution, these values would had been larger. Thus, the calculated values are very approximate, and it is likely that the real fraction of butylammonium ions located within these layers is larger than the given values. In this context it is worth noting that the intrasolution and solution−clay correlations giving rise to the observable peaks in $G(r_z)$ are very weak compared to the total scattering, reflecting the disordered nature of the samples. However, it is important to note that the adsorption does proceed in the direction predicted by electrical theory, with fewer ions adsorbed at the higher salt concentration.

Predictions of ion adsorption[4] of fractions of 90% and 80% for the gels in 0.03 and 0.1 M salt solutions, respectively, were obtained from linear fits to plots of the logarithm of the applied uniaxial stress against the *d* spacing, which should be linear according to both DLVO and Sogami theories.[23] These values are a factor of 2 higher than those given above, but we are at present unable to judge whether this is due to the uncertainties in the quantitative analysis of the diffuse scattering or deficiencies in electrical theory. We are also unable to judge whether or not the ion distribution between the dressed macroions follows the Poisson−Boltzmann distribution implicit in both DLVO and Sogami theories. This information may be contained in the low Q ($Q < 0.2$ Å^{-1}) diffuse scattering, which however is obliterated by the tail of the much stronger Bragg peaks due to the interplatelet correlation. Such limitations do not affect the analysis of the dressed macroion structure.

To conclude, the present neutron diffraction study of butylammonium vermiculite clay gels shows that the interlayer structure of the aqueous solution is effectively independent of the salt concentation *c*, the applied uniaxial stress *p*, and the sol concentration *r* for moderate *p* and *r*. The results give some indications that the lowest achievable *d* spacing at very high pressures or large concentrations is of the order of 35 Å.

Acknowledgment. We thank Christina Line, Christian Rey, and Ron Ghosh of the Institut Laue-Langevin for their help in retrieving data. J.S. thanks the Swedish Natural Science Research Council for a postdoctoral grant, and M.V.S. thanks EPSRC for provision of an Advanced Fellowship to support the work.

References and Notes

(1) Walker, G. F. *Nature* **1960**, *187*, 312.
(2) Smalley, M. V.; Thomas, R. K.; Braganza, L. F.; Matsuo, T. *Clays Clay Miner.* **1989**, *37*, 474.
(3) Braganza, L. F.; Crawford, R. J.; Smalley, M. V.; Thomas, R. K. *Clays Clay Miner.* **1990**, *38*, 90.
(4) Crawford, R. J.; Smalley M. V.; Thomas, R. K. *Adv. Colloid Interface Sci.* **1991**, *34*, 537.
(5) Williams, G. D.; Moody, K. R.; Smalley, M. V.; King, S. M. *Clays Clay Miner.* **1994**, *42*, 614.
(6) Smalley, M. V. *Langmuir* **1994**, *10*, 2884.
(7) Hunter, R. J. *Foundations of Colloid Science*; Clarendon Press: Oxford, 1993; Vol. 1.
(8) Rose, D. A.; Benjamin, I. *J. Chem. Phys.* **1993**, *98*, 2283.
(9) Smalley, M. V.; Schärtl, W.; Hashimoto, T. *Langmuir* **1996**, *12*, 1331.
(10) Swenson, J.; Smalley, M. V.; Thomas, R. K.; Crawford, R. J.; Braganza, L. F. *Langmuir* **1997**, *13*, 6654.
(11) Stern, O. *Z. Elektrochem.* **1924**, *30*, 508.
(12) Derjaguin, B. V.; Landau, L. *Acta Physiochem.* **1941**, *14*, 633.
(13) Verwey, E. J. W.; Overbeek, J. Th. G. *Theory of the Stability of Lyophobic Colloids*; Elsevier: Amsterdam, 1948.
(14) Sogami, I. *Phys. Lett. A* **1983**, *96*, 199.
(15) Sogami, I.; Ise, N. *J. Chem. Phys.* **1984**, *81*, 6320.
(16) McCarney, J.; Smalley, M. V. *Clay Miner.* **1995**, *30*, 187.
(17) Garrett, W. G.; Walker, G. F. *Clays Clay Miner.* **1962**, *9*, 557.
(18) Institut Laue-Langevin, Neutron Research Facilities at the High Flux Reactor, Institut Laue-Langevin, Grenoble, France, 1996.
(19) Norrish, K.; Rausel-Colom, J. A. *Clays Clay Miner.* **1963**, *10*, 123.
(20) Rausel-Colom, J. A. *Trans. Faraday Soc.* **1964**, *60*, 190.
(21) Williams, G. D.; Soper, A. K; Skipper, N. T.; Smalley, M. V. To be published.
(22) Low, P. F. *Langmuir* **1987**, *3*, 18.
(23) Smalley, M. V.; Sogami, I. S. *Mol. Phys.* **1995**, *85*, 869.
(24) Smalley, M. V. *Mol. Phys.* **1990**, *71*, 1251.
(25) Smalley, M. V. *Prog. Colloid Polym. Sci.* **1994**, *97*, 59.